scientific reports

Check for updates

OPEN

Low-resolution FAIMS for increased peptide coverage in low-load and single-cell proteomics

Dominic G. Hoch[1,6], Michael Belford[2], Lilian R. Heil[2], Karl Mechtler[3,4,5]✉ & Manuel Matzinger[3,6]✉

Field Asymmetric Ion Mobility Spectrometry (FAIMS) is an indispensable tool in single-cell and low-input proteomics. Here, we show that tuning FAIMS resolution via electrode temperature modulation improves sensitivity. We demonstrate that lowering FAIMS resolution broadens the compensation voltage window, thereby increasing ion transmission. This significantly improves ion counts, quantitative precision and peptide identifications by 25–34%. These results were mirrored when analyzing single cell samples.

Field Asymmetric Ion Mobility Spectrometry (FAIMS) separates gas-phase ions based on their mobility differences under alternating high and low electric fields at atmospheric pressure. Ions are transported by carrier gas flow between two closely spaced electrodes, with an asymmetric electric field waveform applied orthogonally[1,2]. Ion mobility varies with electric field strength, causing ions to behave differently during the high and low field phases. Ions with equal mobility in both fields pass through the device, while ions with differing mobilities are removed. A small direct current compensation voltage (CV) counterbalances net drift, allowing selective transmission of ions with specific mobility characteristics. FAIMS enhances selectivity and reduces chemical noise, benefiting complex biological samples and single-cell proteomics[3–6]. Unlike other ion mobility separations, FAIMS acts as front-end filter, where ions that are not transmitted at the selected CV are discarded prior to entering instrument. Therefore, FAIMS can improve overall instrument cleaning cycle by filtering out contaminants, but discarding all ions not transmitted at a given CV introduces limitations that include post-switching delay time required with each change of CV, limiting the number of CVs per experiment. Using a single CV during a discovery experiment will increase the signal-to-noise of analytes transmitted at this compensation voltage, enabling new lower abundance peptides to be detected and often increasing protein-level identifications. However, many peptides detectable without FAIMS may not be detectable at this CV and are filtered out, resulting in a decrease in peptide-level identification in many cases. Previous work showed that up to 25% of all precursors found without using FAIMS cannot be identified with FAIMS applying a single CV fraction[6]. Choosing more CVs would increase peptide coverage while maintaining benefits of increased selectivity. However, previous FAIMS-Orbitrap optimizations have demonstrated that increasing the number of CVs lengthens the MS duty cycle (as time for CV switching adds up), which can negatively influence quantitative precision and even coverage and acquiring multiple injections of a single sample each at a different CV is often not feasible due to time and sample constraints[7–9].

The FAIMS electrode temperature significantly influences ion mobility and resolving power and is controlled by a gas stream within FAIMS[2,10]. Temperature control thereby optimizes ion separation, with higher temperatures causing increased ion kinetic energy due to thermal energy being transferred to the ions by more frequent collisions with surrounding gas molecules. The promoted ion–neutral collisions further lead to improved declustering of ion–neutral (e.g., solvent) clusters[11,12]. As a result, the effective collisional cross section is reduced, thereby increasing ion mobility and sharpening FAIMS separations. In practice, this is consistent with the use of heated capillaries and elevated source temperatures upstream of FAIMS to enhance ion desolvation and minimize the transmission of incompletely desolvated droplets into the FAIMS cell. Of note, while elevated kinetic energy generally causes elevated mobility, in some cases ions may unfold at higher temperatures leading to reduced mobility[13]..

[1]Thermo Fisher Scientific, Reinach, Switzerland. [2]Thermo Fisher Scientific, San Jose, CA 95134, USA. [3]Research Institute of Molecular Pathology (IMP), Vienna BioCenter (VBC), Vienna, Austria. [4]Gregor Mendel Institute of Molecular Plant Biology (GMI), Austrian Academy of Sciences, Vienna BioCenter (VBC), Vienna, Austria. [5]Institute of Molecular Biotechnology (IMBA), Austrian Academy of Sciences, Vienna BioCenter (VBC), Vienna, Austria. [6]These authors contributed equally to this work: Dominic G. Hoch and Manuel Matzinger. ✉email: karl.mechtler@imp.ac.at; manuel.matzinger@imp.ac.at

One potentially promising method to increase the performance of FAIMS in a single CV discovery experiment is to optimize the resolving power of the FAIMS separation, balancing selectivity versus total ion transmission to fit the experimental requirements. Although the dimensions of the electrode gap and the amplitude of the RF-waveform (E) are the main factors determining FAIMS separation, electrode temperature significantly influences ion mobility and resolving power by changing the effective field within the gap and is a parameter that can be adjusted on existing commercial hardware. Since ion separation is occurring within a gas bath at atmospheric pressure, the number density (N) must also be considered when determining the FAIMS field that sets both the CV value and peak width of the CV fraction. In standard resolution FAIMS, the inner and outer electrodes are set to the same temperature, often 100 °C. As the temperatures are reduced, the field strength (E/N) is also reduced resulting in a lower CV value (shifted toward zero volts) for the ion fraction. When the electrodes are set independently, the average temperature within the separation gap determines this CV position. However, a thermal gradient across the gap induces a secondary effect affecting the CV peak width when coupled with the non-uniform field between cylindrical electrodes. When the inner electrode is cooler than the outer electrode, the difference in field strength is reduced across the gap resulting in a narrower range of compensation voltages required to transmit the ion fraction. This increases resolution in the CV dimension and is used in targeted analysis to increase selectivity of isobaric molecules. Alternatively, when the outer electrode is cooler than the inner electrode, this effect is flipped so that a broader range of compensation voltages is transmitted. This decreases the FAIMS resolution and increases the fraction of ions per CV that pass through the electrode assembly to the MS. Here, we investigate how changing the outer electrode temperature to lower resolution impacts overall performance in a bottom-up proteomics discovery experiment.

Results

Evaluation of FAIMS resolution effect using selected ions in a static spray

Firstly, we assessed whether CV resolution changes with electrode temperature by directly injecting Pierce™ FlexMix™ Calibration Solution (Thermo Fisher Scientific) into the MS with FAIMS attached and determining the optimum CV values for hexamethoxphosphazene (322.0481 *m/z*), MRFA (*m/z* 524.2655), Hexakis(2,2-difluoroethoxy)phosphazene (622.0289 *m/z*) and Hexakis(2,2,3,3-tetrafluoropropoxy)phosphazene (922.0098 *m/z*) for different outer electrode temperatures (Fig. 1A-D). Standard resolution (T_{inner}: 100 °C, T_{out}: 100 °C) showed narrower peaks than *low-resolution* (T_{inner}:100 °C, T_{out}: 80 °C), with *low-resolution* transmitting ions over a wider CV range (Fig. 1E) and shifting apex CVs slightly toward more positive values (Fig. 1F). This further results in a broader peak area under the curve, indicating increased ion transmission calculated over the entire CV range (Fig. 1G). Notably, for ions 524.2655 *m/z* and 622.0289 *m/z* (Fig. 1B, C), lowering FAIMS resolution further improved transmission at their apex CV which is increased by 18% and 21% for *m/z* 524.2655 and 622.0289 respectively.

Impact on identification numbers and data quality

To assess how FAIMS electrode temperature affects data quality, we injected 250 pg HeLa digest and decreased the outer electrode from 100 °C to 80 °C in 5 °C steps. Protein identifications showed no clear trend or improvement of identification numbers with lowered FAIMS resolution (Fig. 2A), whereas peptide identifications increased progressively with lower temperatures, peaking at 80 °C: 28,063 peptides at standard vs. 35,258 at 80 °C (+25.6%) (Fig. 2B). Moreover, summed protein quantity also rose as the outer electrode temperature decreased (Fig. 2C), and total LC peak fragment ion counts were higher with low-resolution FAIMS than standard settings in 250 pg runs (Supplemental Fig. 1).

This beneficial trend likely extends below 80 °C, but we could not stably reach or maintain 75 °C or lower. The probable cause is the large temperature differential: cooling gas first flushes the 100 °C inner electrode, preventing stable control of the outer electrode at ≤75 °C. We therefore set the minimum outer temperature to 80 °C, which we could reproducibly maintain over the entire gradient (Supplemental Fig. 2).

Encouraged by these results, we tested dependence on peptide load by running a HeLa digest concentration series (250 pg–16 ng) comparing the standard electrode temperature to the lowest outer electrode setting (80 °C). Guided by the 250 pg data, we also adjusted DIA window width and maximum isolation time (maxIT) per load to exploit the higher ion flux with *low-resolution* FAIMS. Lowering the outer electrode to 80 °C increased peptide identifications by 14–34% for all loads (Fig. 3B). Notably, smaller DIA windows further boosted peptide IDs with low-resolution FAIMS, whereas they generally reduced- IDs with standard resolution. Because low-resolution FAIMS increases ion-flux, shorter maxITs- suffice, enabling narrower DIA windows and higher selectivity. Across the series, protein groups were also higher with low vs. standard---resolution (~1–10%), though less than at the peptide level (Fig. 3A). The largest gain occurred at 250 pg with 10 Th windows and 20 ms: 5457 vs. 4923 protein IDs (+10%) and 39,451 vs. 25,895 peptide IDs (+34%). Sensitivity gains did not cause major changes in peptide characteristics, with only a slight shift in the median precursor *m/z* observed and unaltered retention time distribution (Fig. 4A-B). In line with the m/z shift, a slight shift in precursor charge distribution towards +3 charged was observed: 21% vs. 25% of all identified precursors are z = 3 at an outer electrode temperature of 100 vs. 80 °C respectively (250 pg, Supplemental Fig. 3). The observed trend of lowered FAIMS resolution slightly favoring +3 charged ions to pass the FAIMS electrode was confirmed for higher inputs of up to 16 ng (Fig. 4C). Of note, independently from FAIMS resolution, a slightly increased relative fraction of identified +3 and higher charged precursors was further observed with growing input amount (Fig. 4C). We hypothesize, that higher charged precursors are less abundant compared to the predominant +2 charged species in our tryptic digests, which is why both, higher input amount as well as improved sensitivity by lowered FAIMS resolution improves their detectability and hence its yielded protein quantity was consistently higher with decreased outer electrode temperature (Fig. 3C), and together with a higher median contribution to total LC peak fragment ion count (Supplemental Fig. 1), indicates improved quantitative precision via lower

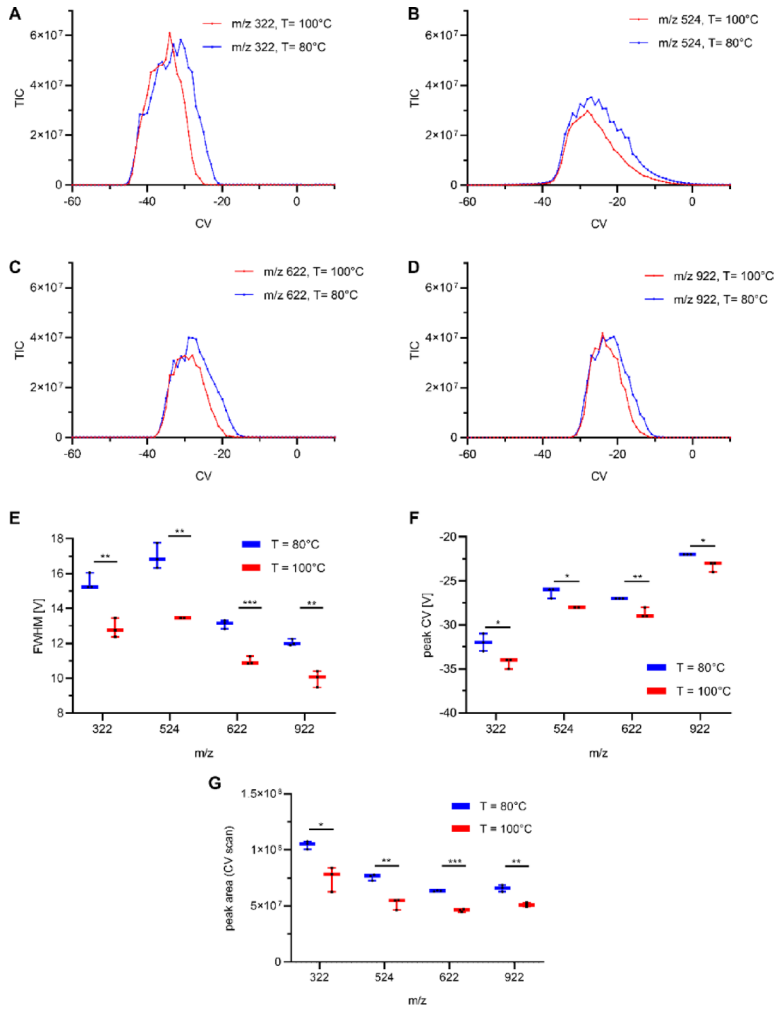

Fig. 1. FAIMS resolution assessed by FlexMix injection. TICs from SIM scans upon FlexMix injection with standard resolution (T_{outer} electrode = 100 °C) vs. low resolution (T_{outer} electrode = 80 °C) during CV scan for m/z 322.0481 (**A**), 524.2655 (**B**), 622.0289 (**C**) and 922.0098 (**D**). One representative replicate of 3 technical replicates is shown. **E**: Box plots of peak full width half maximum (FWHM) across CV scans, **F**: peak apex CV, and **G**: peak area from CV scan. All box plots show medians with SD error, $n = 3$. **E-G**: Significance based on a two-tailed unpaired students t-test is given as follows: * = $P < 0.05$, ** = $P < 0.01$, *** = $P < 0.001$, $n = 3$.

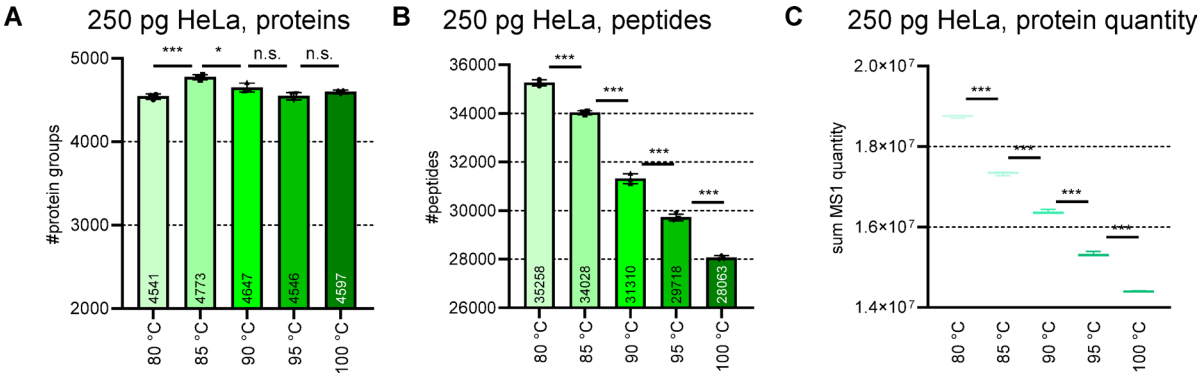

Fig. 2. Influence of FAIMS electrode temperature on protein and peptide identifications and their quantities. Bars show averages with SD error bars, $n = 3$ technical replicates. Unpaired two tailed students t tests were performed, with ***$p < 0.001$, **$p < 0.01$, *$p < 0.05$ and n.s. $p \geq 0.05$. **A**: Proteins identified in 250pg HeLa, **B**: Peptides identified in 250pg HeLa, **C**: Average sum of protein quantity (MS1 level).

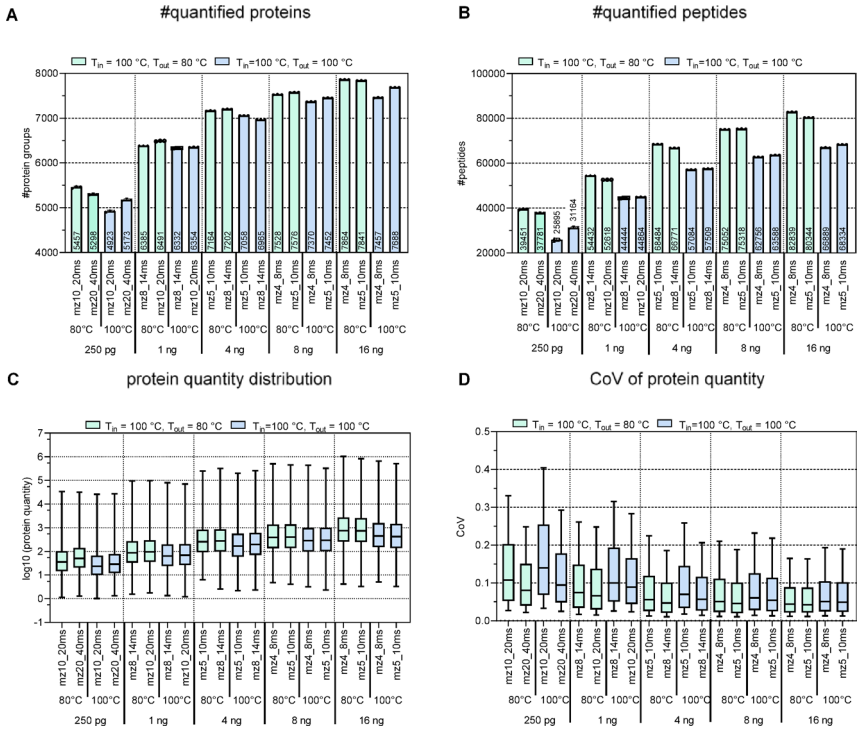

Fig. 3. Titration of input amounts at altered FAIMS resolution. Diluted HeLa digests were injected at indicated amounts. Bars show averages with SD error bars; $n = 3$ technical replicates. Unpaired two tailed Student's T-Test: *** $p < 0.001$, ** $p < 0.01$, * $p < 0.05$, n.s. $p \geq 0.05$. Given mz values indicate the DIA isolation windows and subsequent numbers indicate the maximum injection time in ms. Plots show the number of quantified proteins (**A**) and peptides (**B**) as well as quantity distributions as box plots with min-max whiskers (**C**) and protein quantity CoVs as box plots with 10–90% percentile whiskers for proteins quantified in $n = 3$ replicates (**D**).

coefficients of variation (CoVs) across all inputs (Fig. 3D). To that end, lowering FAIMS resolution mostly leads to additional peptide identifications, while less than 9% of peptides quantified at standard resolution were not found at lowered resolution (Supplemental Fig. 4 A). At protein level less than 6% were found only at standard resolution (Supplemental Fig. 4B).

Impact of FAIMS resolution on single cell proteomic samples

We moved forward by analyzing single cells to determine if the electrode temperature also positively influences the measurement of actual single cells. H460 cells were prepared using the previously published OnePot workflow[14]. Here, we observed the same pattern as in the HeLa dilution series: Protein (+4%) and peptide identifications (+21%) as well as the protein quantities improved with *low-resolution* FAIMS (Fig. 5A-C). In line with the observations made for HeLa dilutions, the overlap of quantified peptides and proteins is close to 100%, with mostly additional peptides added at low resolution FAIMS (Supplemental Fig. 5). We included 0-cell control runs containing identical components to single cell samples and that were processed in the exact same way on the same 384-well plate, but with no cell isolated into the respective well. Their IDs originate from background signals, i.e. contaminations and the added protease itself. Clearly, lowering the resolution improves sensitivity, crucial for single cell proteomic applications. This yields differences in the obtained proteomic fingerprint, comparable to a batch effect, leading to distinct populations of cells within a PCA plot depending on the electrode temperature (Fig. 5D).

Discussion

This study demonstrates that *low-resolution* FAIMS significantly increases peptide and protein identifications from low-load samples. By broadening the compensation voltage window, it enhances ion transmission, improving identifications in low-load HeLa digests and single cells. In line, higher charged and higher m/z ions showed an improved identification rate compared to standard resolution FAIMS. The resulting sensitivity boosts detection of low-abundance proteins and strengthens quantification quality, which is crucial for single-cell proteomics.

Low-resolution FAIMS also raises ion counts in MS1 and MS2, improving quantitative precision, we consistently observed lowered CoVs of samples measured with a lower outer electrode temperature.

These findings provide a simple, practical tweak: adjusting FAIMS resolution delivers better results without additional hardware or changes to data processing, making it a cost-effective, straightforward enhancement.

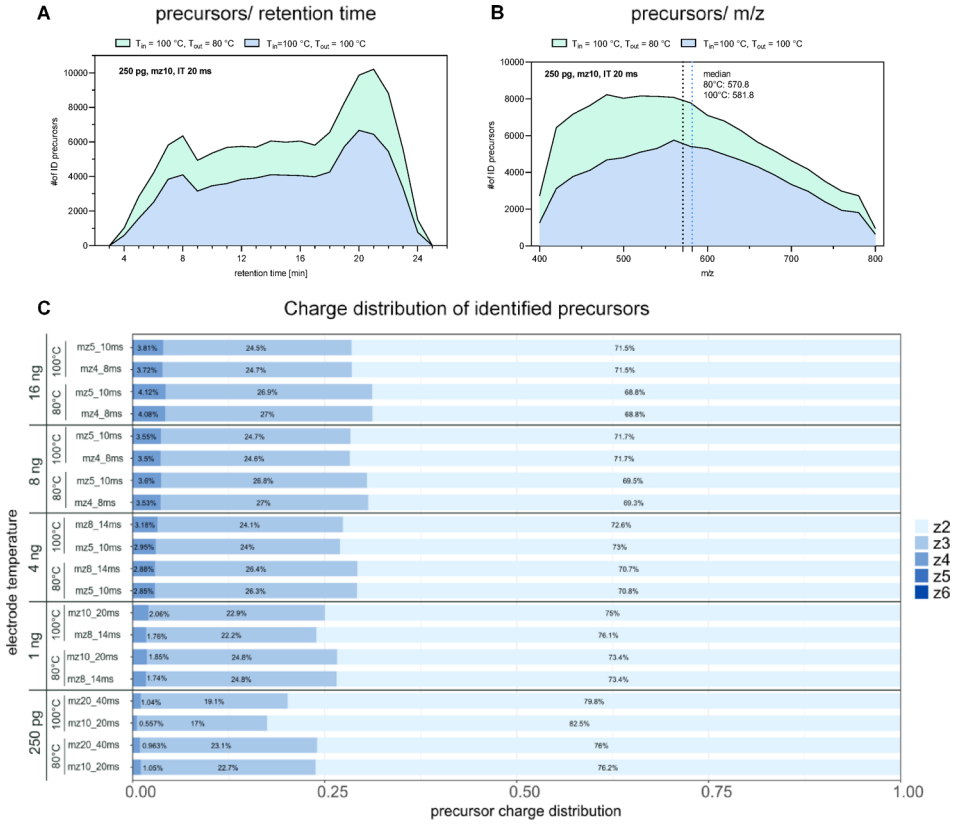

Fig. 4. Precursor characteristics upon altering FAIMS resolution. **A**: Precursor retention time distribution (250 pg HeLa), **B**: m/z distribution (250 pg HeLa) over retention time and **C**: charge distribution at given input are shown. Isolation window size (given as mz) and injection time (given in ms) were aligned to input. Precursors of higher charges of $z > 3$ were present as given in the legend but at < 0.1% prevalence, which is why they are not displayed in the plots due to limited space.

Methods

Cultivation of H460 cells

H460 cells were a kind gift from the group of Josef Penninger (IMBA, Vienna). Their original commercial source is ATCC. Cells were cultured as described earlier[6]. To recapitulate, cells were grown at 37 °C in a humidified atmosphere at 5% CO_2. H460 cells were grown in RPMI 1640 medium. Cell medium was supplemented with 10% fetal bovine serum (FBS; 10270, Fisher Scientific), 1× penicillin–streptomycin (P0781-100ML, Sigma-Aldrich), 100× l-glutamine (200 mM, 250030-024, Thermo Scientific) and 1 mM sodium pyruvate (for RPMI only; 4275, Sigma-Aldrich). Cells were grown to around 75% confluency before trypsinization with 0.05% Trypsin-EDTA (25300-054, Thermo Scientific), followed by washing three times with PBS. Cells were resuspended in PBS at a density of 200 cells/µl for isolation using the cellenONE (Cellenion).

Single cell proteomic sample preparation

Individual cell isolation, lysis and digestion were performed within a 384-well plate (Eppendorf twin.tec PCR Plate 384 LoBind) using the cellenONE robot based on our previously published One-Pot protocol[14]. The cellenONE robot was operated using its control software (v2.0–1146). Cells were sorted into wells containing 1 µl of master mix (0.2% DDM (D4641-500MG, Sigma-Aldrich), 100 mM triethylammonium bicarbonate (TEAB; 17902-500ML, Fluka Analytical), 3 ng μl^{-1} trypsin (Trypsin Gold, V5280, Promega) and 1% DMSO). Humidity and temperature were controlled at 50% and 15 °C during cell sorting. H460 cells were isolated at a given diameter of 20–35 µm. The maximum elongation was set to 1.6. Cell lysis and protein digestion were performed at 40 °C and 70% relative humidity for 30 min before an additional 500 nl of 3 ng μl^{-1} trypsin was added for an additional 1.5 h. After lysis and digestion, 3.0 µl of 0.1% TFA was added to the respective wells for quenching and storage at − 20 °C. For LC–MS/MS analysis, samples were directly injected from the 384-well plate.

Diluted bulk digests

HeLa (Thermo Scientific, Pierce HeLa Protein Digest Standard, 88328) peptides were dissolved in 0.1% TFA and 0.015% DDM (D4641-500MG, Sigma-Aldrich) at a concentration of 5 ng μl^{-1} for injection into the LC–MS system. Injection amounts were adopted from 0.05 µL to 3.2 µL to inject sample amounts ranging from a single cell equivalent (250 pg) – 16 ng respectively.

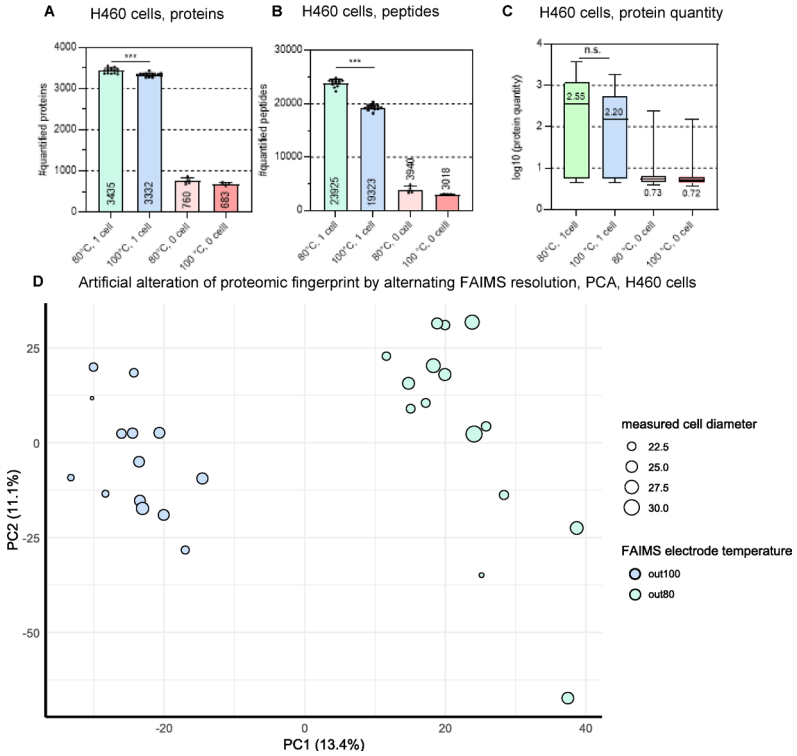

Fig. 5. Single H460 cells analyzed at high vs. low FAIMS resolution. (**A–B**): Bars show average quantified protein groups (**A**) and peptides (**B**) per cell; error bars are SD; individual cells shown as black dots. (**C**) Box plots of protein quantity distributions (10–90% percentile) for single cells and 0-cell controls. Missing values were filtered; data not normalized. (**D**) PCA; each dot represents a single H460 cell measured at the indicated FAIMS electrode temperature; dot size reflects cell diameter. $N = 14$ cells for 100 °C and 80 °C; $n = 5$ for 0-cell controls.

LC–MS analysis

Samples were analyzed using the Thermo Scientific Vanquish Neo UHPLC system. Thermo Tune software version 1.1.477.46 or higher was used to acquire data. Peptides were loaded on a trapping column (Thermo Fisher Scientific, PepMap C18, 5 mm × 300 µm i.d., 5 µm particles, 100 Å pore size) using 0.1% TFA for the loading buffer. Peptides were separated on an Aurora Rapid™ 8 × 75 XT C18 nanoflow UHPLC column with an integrated emitter (Ion Optics) at 50 °C. Peptide separation was performed at 50–80 with details provided in Supplementary Tables 1 and with all single-cell measurements performed at 80 SPD.

For MS measuring, the Orbitrap Astral mass spectrometer (Thermo Scientific) equipped with a FAIMS Pro Duo interface (Thermo Scientific) and an EASY-Spray source was coupled to the LC. A compensation voltage of − 48 V and a carrier gas flow of 3.5 L/min was chosen based on previous results[6]. An electrospray voltage of 1.9 kV was applied for ionization and adopted to slightly higher voltages for aged emitters to ensure spray stability.

MS method settings used were based on previous work[6]. In brief, MS^1 spectra were recorded using the Orbitrap analyzer at a resolution of 240,000 from *m/z* 400 to 900 using an automatic gain control (AGC) target of 500% and a maximum injection time of 100 ms. MS2 scans were acquired in the Astral analyzer, the precursor range was set to 400–800 *m/z* and the AGC target to 500%. Single cells were measured with DIA window size of 20 Th and maxIT 40 ms. The Hela dilution series were acquired with optimized method parameters based on the peptide load on column. The DIA isolation widths and maxIT were adjusted as specified in the respective graphs.

Data analysis

Basic steps of data analysis were performed as described earlier[6] with the following details: All raw data were analyzed using Spectronaut (version 20.1, Biognosys). Data from diluted bulk samples was searched using directDIA + in method evaluation mode allowing for cross normalization within each tested condition. Single cell data was searched in directDIA+ mode. Quantification was performed at the MS^1 level and a minimum quantity filter of 10 was applied to single cell data to remove noisy quantification results. Unless otherwise indicated, default settings were used, with carbamidomethylation of cysteines as a static modification removed for single cell searches as no alkylation step was performed. Searches were performed against the human proteome (UniProt proteome UP000005640, reviewed, 20,408 protein entries, downloaded 4th of August 2023) and the CRAPome[15](118 protein entries). If not otherwise stated, FDR filtering was based on default settings of Spectronaut and at 1% at the protein level. Post processing was done using R and Graph Pad Prism (v8.1.1). For PCA no additional normalization was applied, and NaN values were replaced with 0.

The LC peak total ion counts from 250pg HeLa 50SPD runs were extracted using Skyline (v25.1.0.142)[16] using the ion count report as used by Hsu et al.[17]

Data availability

The MS raw proteomics data and Spectronaut search results have been deposited to the ProteomeXchange Consortium[18] via the PRIDE partner repository with the dataset identifier PXD069335.

Received: 19 November 2025; Accepted: 17 March 2026
Published online: 21 March 2026

References

1. Levin, D. S., Miller, R. A., Nazarov, E. G. & Vouros, P. Rapid separation and quantitative analysis of peptides using a new nanoelectrospray- differential mobility spectrometer-mass spectrometer system. *Anal. Chem.* **78**, 5443–5452 (2006).
2. Barnett, D. A., Belford, M., Dunyach, J. J. & Purves, R. W. Characterization of a Temperature-Controlled FAIMS System. *J. Am. Soc. Mass. Spectrom.* **18**, 1653–1663 (2007).
3. Zheng, R. et al. A High-Sensitivity Low-Nanoflow LC-MS Configuration for High-Throughput Sample-Limited Proteomics. *Anal. Chem.* **95**, 18673–18678 (2023).
4. Schoof, E. M. et al. Quantitative single-cell proteomics as a tool to characterize cellular hierarchies. *Nat. Commun.* **12**, 3341 (2021).
5. Furtwängler, B. et al. Real-Time Search-Assisted Acquisition on a Tribrid Mass Spectrometer Improves Coverage in Multiplexed Single-Cell Proteomics. *Mol. Cell. Proteom.* **21**, 100219 (2022).
6. Bubis, J. A. et al. Challenging the Astral mass analyzer to quantify up to 5,300 proteins per single cell at unseen accuracy to uncover cellular heterogeneity. *Nat. Methods*. 1–10. https://doi.org/10.1038/s41592-024-02559-1 (2025).
7. Bekker-Jensen, D. B. et al. A Compact Quadrupole-Orbitrap Mass Spectrometer with FAIMS Interface Improves Proteome Coverage in Short LC Gradients. *Mol. Cell. Proteom. MCP.* **19**, 716–729 (2020).
8. Matzinger, M. et al. Micropillar arrays, wide window acquisition and AI-based data analysis improve comprehensiveness in multiple proteomic applications. *Nat. Commun.* **15**, 1019 (2024).
9. Hebert, A. S. et al. Comprehensive Single-Shot Proteomics with FAIMS on a Hybrid Orbitrap Mass Spectrometer. *Anal. Chem.* **90**, 9529–9537 (2018).
10. Shvartsburg, A., Anderson, A. A., Smith, D. & G. & Pushing the Frontier of High-Definition Ion Mobility Spectrometry Using FAIMS. *Mass. Spectrom.* **2**, S0011 (2013).
11. Swearingen, K. E. & Moritz, R. L. High Field Asymmetric Waveform Ion Mobility Spectrometry (FAIMS) for Mass Spectrometry-Based Proteomics. *Expert Rev. Proteom.* **9**, 505–517 (2012).
12. Krasnova, K., Creaser, C. S. & Reynolds, J. C. Determination of Collisional Cross Section Using Microscale High-Field Asymmetric Waveform ion Mobility Spectroscopy–Mass Spectrometry (FAIMS-MS). *Rapid Commun. Mass. Spectrom.* **39**, e10010 (2025).
13. Robinson, E. W., Shvartsburg, A. A., Tang, K. & Smith, R. D. Control of Ion Distortion in Field Asymmetric Waveform Ion Mobility Spectrometry via Variation of Dispersion Field and Gas Temperature. *Anal. Chem.* **80**, 7508–7515 (2008).
14. Matzinger, M., Müller, E., Dürnberger, G., Pichler, P. & Mechtler, K. Robust and Easy-to-Use One-Pot Workflow for Label-Free Single-Cell Proteomics. *Anal. Chem.* **95**, 4435–4445 (2023).
15. Mellacheruvu, D. et al. The CRAPome: a contaminant repository for affinity purification–mass spectrometry data. *Nat. Methods.* **10**, 730–736 (2013).
16. Pino, L. K. et al. The Skyline ecosystem: Informatics for quantitative mass spectrometry proteomics. *Mass. Spectrom. Rev.* **39**, 229–244 (2020).
17. Hsu, C. et al. Evaluation of a prototype Orbitrap Astral Zoom mass spectrometer for quantitative proteomics – Beyond identification lists. 05.30.657132 Preprint at (2025). https://doi.org/10.1101/2025.05.30.657132 (2025).
18. Perez-Riverol, Y. et al. The PRIDE database and related tools and resources in 2019: improving support for quantification data. *Nucleic Acids Res.* **47**, D442–D450 (2019).

Acknowledgements

The authors thank the group of Josef Penninger at IMBA for providing H460 cells.

Author contributions

DGH and MM conceptualized the study, designed, and performed experiments, data analysis, and wrote the manuscript. KM supervised the study. MM performed revision work during peer review. MB and LRH helped with technical details on FAIMS during revision. All authors revised and agreed on the final manuscript.

Funding

This work was supported by the infrastructure funding 4th call 2022/01 (AT-SCP) of the Austrian Research Promotion Agency (FFG).

Declarations

Competing interests

DGH, MB and LRH are employees of Thermo Fisher Scientific, the other authors declare no competing financial interests.

Additional information

Supplementary Information The online version contains supplementary material available at https://doi.org/10.1038/s41598-026-45228-3.

Correspondence and requests for materials should be addressed to K.M. or M.M.